Memory entrainment by visually evoked theta-gamma coupling in the human brain

Moritz Köster[1,2]*, Ulla Martens[2], & Thomas Gruber[2]

[1]Free University Berlin, Institute of Psychology, Habelschwerdter Allee 45, 14195 Berlin, Germany

[2]Osnabrück University, Institute of Psychology, Seminarstraße 20, 49074 Osnabrück, Germany

Corresponding author:
Moritz Köster
Free University Berlin
Institute of Psychology
Habelschwerdter Allee 45
14195 Berlin
Germany
E-mail: moritz.koester@fu-berlin.de

Abstract

The formation of novel memories is orchestrated by the rhythmic interplay of neuronal activity within and across cell assemblies. Critically, given the correlative nature of neurophysiological recordings, the functional role of neuronal rhythms in the human brain is still unclear. Here, episodic memory encoding was entrained by a rhythmic visual stimulation at an individually adjusted theta frequency (3-8Hz), in contrast to the stimulation at an individual alpha frequency (8-12Hz). Memory enhancing effects of the theta stimulation were not explained by theta power *per se*, but were driven by theta coupled gamma oscillations (40-120Hz) in wide spread neocortical networks. These findings provide first evidence for a functional role of the theta-gamma neuronal code in human episodic memory. The entrainment of mnemonic network mechanisms by a simplistic visual stimulation technique demonstrates that internal rhythms can align with external pacemakers, which can entrain complex cognitive functions in the wake human brain.

Introduction

It is a continuous task of the wake human brain to integrate novel information from the environment, to sustain a coherent internal representation of the outer world (Buzsáki, 1996; Kandel et al., 2013). How is this complex function achieved and which are the functional mechanisms underlying this mnemonic processes within the neuronal networks of the human brain? Rhythmic activity coordinates and integrates distributed processes within and across nerve cell populations (Engel et al., 2001; Fries, 2015; Varela et al., 2001). This may allow a real-time integration of novel experiences into existing neuronal networks (Fell and Axmacher, 2011; Hanslmayr et al., 2016) accompanying perceptual processes (Cowan, 1988).

In subsequent memory paradigms, the neuronal activity during encoding is contrasted between later remembered and later forgotten items (Paller and Wagner, 2002) to isolate the neuronal processes underlying memory formation. This line of research has established a close association between the formation of novel memory traces and neuronal oscillations in the theta (3-8 Hz), alpha (8-12 Hz) and gamma (30-90 Hz) frequency in the human brain (Friese et al., 2013; Klimesch, 1999; Osipova et al., 2006). Specifically, successful encoding of visual stimuli was marked by increases in theta and gamma power and a decrease in alpha power (Friese et al., 2013; Osipova et al., 2006).

Theta oscillations are proposed to serve the ordering and binding of perceptual information, which are reflected in the gamma band oscillations (Bahramisharif et al., 2017; O'Keefe and Recce, 1993), and form a theta-gamma neuronal code (Lisman and Jensen, 2013). This is substantiated by theta-gamma phase-amplitude coupling (PAC) in the human neocortex (Canolty et al., 2006), which increased during successful memory encoding in neocortical and medio-temporal networks (Friese et al., 2013; Heusser et al., 2016; Staudigl and Hanslmayr, 2013). The theta-gamma code is assumed to facilitate the integration of perceptual information into existing networks by squeezing real time events onto a neuronal time scale (Buzsaki, 2004), a precondition for long-term potentiation processes in the hippocampus (Pavlides et al., 1988), the core system of episodic memory in the mammalian brain (Eichenbaum, 2004; Squire and Zola-morgan, 1991). Reduced alpha oscillations during successful encoding may reflect attention gating processes that facilitate memory encoding (Jensen and Mazaheri, 2010; Klimesch, 2012).

Critically, empirical findings that fuel contemporary theoretical models on distinct roles of neuronal theta, alpha and gamma oscillations in mnemonic processes are merely correlational. This is, oscillatory activity observed in the human brain could be an epiphenomenal byproduct of neuronal network processes, without functional relevance

(Buzsaki, 2004). There is first evidence that memory consolidation processes during sleep can be entrained by transcranial alternating currents (Marshall et al., 2006) and auditory stimulation (Ngo et al., 2013) in a slow-wave rhythm (0.5 – 2 Hz). Yet, evidence for the functional relevance of oscillatory dynamics during memory encoding in the wake human brain is still lacking.

In the present study, we experimentally manipulated the memory encoding processes by presenting visual stimuli at an individually adjusted theta rhythm to selectively enhance the memory encoding process, compared to a stimulation at an individual alpha frequency. A scalp recorded electroencephalogram (EEG) was assessed to scrutinize entrained theta, alpha and phase-amplitude coupling (PAC) dynamics underpinning successful memory encoding.

Results

Visual theta stimulation enhances memory encoding by theta SSVEP in neocortical networks

Subjects (n = 20) saw visually flickering stimuli, presented at an individual theta or alpha frequency, using the duty-cycles (i.e., on and off screens) of an CTR monitor (Figure 1A). A pre-study was conducted to adjust theta and alpha frequencies individually (Friese et al., 2013), due to high inter-individual variations in the theta and the alpha frequency (Klimesch, 1999). We further presented static stimuli to estimate the difference in memory performance for flickering and non-flickering stimuli. In a retrieval session, we assessed how the experimental manipulation of the encoding process effected subjects subsequent memory performance (SME = percent of subsequently remembered [SR] minus subsequently forgotten [SF] items).

The stimulation at an individual theta frequency increased subsequent memory performance (SME), compared to the alpha stimulation, $t(19) = 2.24$, $p = .018$, one-sided. This was due to higher number of SR items for theta, as well as a higher rate of SF items for alpha (see Figure 1B; 23.8 % vs. 21.5 %, $t(19) = 2.13$, $p = .046$, and 47.4 % vs. 49.9 %, $t(19) = 1.99$, $p = .062$). Static pictures were remembered best (SR: 28.2 % and SF: 42.6 %), with a higher SME than theta, $t(19) = 4.15$, $p < .001$, and alpha, $t(19) = 10.97$, $p < .001$. SSVEP stimulation did not affect the rates of subsequent know (SK) responses (theta: 28.7 %, alpha: 28.6 %, gamma: 29.3 %). Note that the mean differences for SR and SF were calculated post hoc, following significant main effects and interactions in the overall ANOVA (3 Conditions [theta, alpha, gamma] x 3 Responses [SR, SK, SF]) and the subsidiary ANOVAs, for the three responses, all *p*s < .001, but not for SK responses (reported above).

Visually flickering stimuli elicit steady state visually evoked potentials (SSVEPs, see Figure 1C), visible in the scalp recorded EEG (Müller et al., 2003). A SSVEP is the oscillatory response of the visual cortex to a rapidly repeating (flickering) stimulus, at the specific frequency of the driving stimulus. Here, the neuronal responses to the visual theta and alpha stimulation were assessed by a 128 scalp EEG electrodes, to analyze the oscillatory dynamics underlying visual memory entrainment.

The theta and the alpha stimulation elicited clear SSVEP signals over the visual cortex, accompanied by increased gamma oscillations at posterior recording sites, all $t(19) > 3.11$, $p < .006$. In a next step, we tested if inter-individual differences in memory entrainment (theta SME – alpha SME) were driven by memory enhancing effects of the theta stimulation or by disrupting effects of alpha stimulation. Memory entrainment was clearly predicted by the power and spread of the theta SSVEP, $r = .71$, $p = .00043$, $R^2 = .50$ (see Figure 1D; power at the peak electrode and the spread of the SSVEP signal, determined by the entropy), but not by the alpha SSVEP signal, $r = .09$, $p = .697$. That is, inter-individual differences in memory entrainment were explained by the responsiveness of subjects' cortical networks to the theta SSVEP stimulation. Thus, memory entrainment was driven by the theta stimulation, but not by disrupting effects of the alpha stimulation.

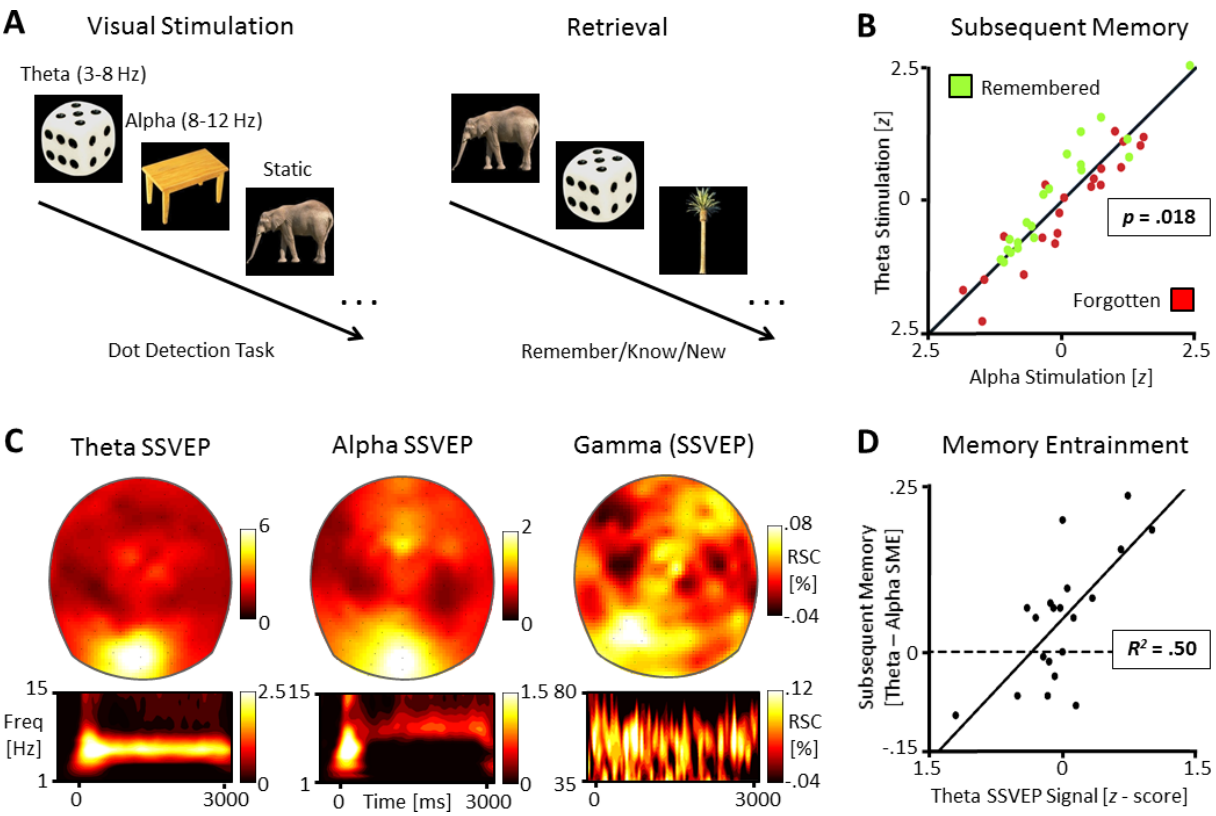

Figure 1 Study design and visual stimulation results. (A) Object pictures were presented at different stimulation frequencies, an individually adjusted theta (3-8 Hz), or alpha (8-12 Hz) frequency, or static (non-flickering). (B) Subsequently remembered (SR) and subsequently forgotten (SF) response rates (z-standardized for the combined visualization). Overall subsequent memory performance (SME = SR - SF) was higher for theta, compared to alpha (p = .018, one-sided). Each subject is represented by a green and a red dot; Green dots above the diagonal indicate subjects with a higher SR rate for theta, red dots below the diagonal indicate subjects with a higher SF rate for alpha. The 45° diagonal corresponds to equal response rates for theta and alpha. (C) Topographies of steady state visually evoked potentials (SSVEP) at individual theta and alpha frequencies. The gamma topography displays the 50–80 Hz activity accompanying theta and alpha stimulation. Values indicate relative signal change (RSC, 500-3000ms). Time-frequency plots display the spectral power at the corresponding peak electrode. (D) Inter-individual differences in memory performance theta – alpha (SME) were explained by the power and spread of the theta SSVEP (integrated z-score, r = .71, p = .00043, R^2 = .50), but not by alpha SSVEP (p = .697; not displayed). The diagonal is the regression line.

Memory enhancing effects of theta stimulation are driven by theta coupled gamma oscillations

Theta oscillations showed an inverse SME, namely higher theta SSVEPs for SF, than SK, than SR stimuli, at the peak electrode (Figure 2A, upper panel), $F(2, 38) = 6.41$, $p = .004$. This effect was distributed across posterior, central and frontal regions (Figure 2A, lower panel). The memory enhancing effect of the theta stimulation was resolved by the theta-gamma PAC analyses, testing the coupling between phase of the individual theta SSVEP, at the theta peak electrode, and the 50-80Hz gamma amplitude (Figure 2B), at all 128 electrodes, using the modulation index (MI) (Canolty et al., 2006). The averaged MI cross all 128 electrodes, revealed much higher theta-gamma PAC for SR, compared to SK, compared to SF stimuli, $F(2, 38) = 8.08$, $p < .001$. This main effect peaked over left temporal and centro-frontal electrodes (Figure 2B) indicating that theta-gamma PAC was spread in broad neocortical networks.

Further inspection of theta-gamma PAC revealed that the SME in theta-gamma PAC was not restricted to the preselected gamma frequency range (50-80Hz), but was present across a broad low to high gamma range, from 40-120Hz (Figure 2C). We further inspected the critical theta phase of theta-gamma PAC for successful memory encoding at left temporal recording sites. The gamma amplitude for SR stimuli, compared to SF stimuli, was specifically high at the beginning of the theta phase (0°-90°), corresponding to the onset of the flickering stimulus, but lower towards the end of the on-phase of the flickering stimulus (120°-210°; Figure 2D).

In the control analyses, no SMEs were found at the peak electrode of alpha SSVEPs, $F(2, 38) = 0.74$, $p = .486$, and the gamma power accompanying the SSVEP conditions (Figure 1C), tested in an ANOVA with all subsequent responses (SR, SK, SF) and both SSVEP conditions (theta and alpha), all ps > .634, for all main effects and interactions. In addition, across all conditions and all electrodes, theta-gamma PAC was much higher than alpha-gamma PAC, $t(19) = 3.53$, $p = .002$. Thus, subsequent memory performance was not explained by alpha SSVEPs or the accompanying gamma power.

To conclude, theta SSVEPs were higher for SF compared to SR stimuli, whereas theta-gamma PAC was higher for SR compared to SF stimuli. Thus, the memory enhancing effect of theta stimulation was not explained by theta SSVEP power *per se*, but by theta-gamma PAC processes. Note that the inverse SME for theta power (SF > SR) rules out the possibility that the positive SME in theta-gamma PAC (SR > SF) could be explained by differences in theta SSVEPs power between conditions.

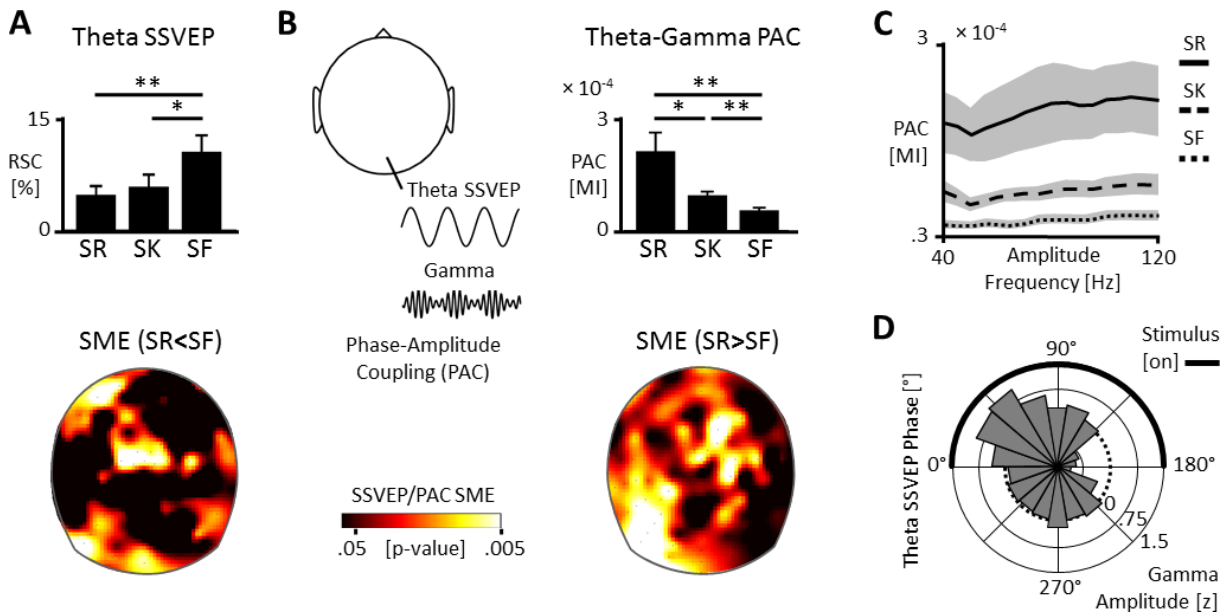

Figure 2 Memory entrainment by theta-gamma coupling. (A) Bars indicate the theta SSVEP signal differences between subsequently remembered (SR), known (SK), and forgotten (SF) items, at the peak electrode (ANOVA: $F[2, 38] = 6.41$, $p = .004$). The topographical map illustrates the distribution of the inverse subsequent memory effect (SME, SF > SR) across the scalp. Note that alpha SSVEP and gamma did not differ between conditions at the peak electrode. (B) The cartoon head illustrates theta-gamma phase amplitude coupling, as assessed by the modulation index (MI). Bars the differences in the MI averaged across all 128 electrodes, i.e., the coupling between the 50-80Hz gamma amplitude at each electrode to the individual theta SSVEP phase at the peak electrode ($F[2, 38] = 8.08$, $p < .001$). The topographical map displays the distribution of the SME (SR > SF) in theta-gamma PAC across the 128 scalp electrodes. Note that overall theta-gamma PAC was much higher than overall alpha-gamma PAC ($p < .002$, not displayed). (C) Theta-gamma PAC across the 40-120Hz gamma range. MI values indicate the mean PAC between gamma amplitude at each of 128 electrodes to the individual SSVEP theta phase at the peak electrode. (D) The circular histogram displays subsequent memory differences (SR-SF) for z-standardized gamma amplitudes at the left temporal peak electrodes of the MI difference plot. All bar plots: *$p < .05$, **$p < .01$.

Discussion

The present results provide first evidence for a functional role of the theta rhythm and the theta-gamma neuronal code in human episodic memory (Lisman and Jensen, 2013). Theta stimulation selectively improved context-dependent, associative memories (SR, “remember” responses), but not familiarity based memory processes (SK, “know” responses) (Tulving, 1995). Critically, memory entrainment by theta stimulation was not explained by the theta power *per se*, but by theta-gamma PAC in distributed neocortical networks. Theta oscillations in the cerebral cortex are associated with mnemonic control processes, namely the ordering and maintenance of perceptual information, reflected in gamma bursts, nested in the theta phase (Bahramisharif et al., 2017; Heusser et al., 2016; Lisman and Jensen, 2013; O’Keefe and Recce, 1993).

The alpha SSVEP stimulation was associated with a lower memory performance, than the theta stimulation. However, the alpha SSVEP signal did not explain inter-individual differences in memory entrainment and did not dissociate between encoding conditions (SR, SK, SF). Furthermore, the alpha SSVEP did not elicit phase coupled gamma oscillations (alpha gamma PAC), when compared to theta-gamma PAC. Thus, the effect of alpha SSVEPs was much less specific compared to the visually entrained theta rhythm and theta-gamma PAC pattern. Theta stimulation did not enhance memory encoding compared to static, non-flickering stimuli. This may be due to the physically longer presentation time (no off frames), or because, in the absence of external stimulation, the brain could establish an optimal rhythmicity itself.

While the theta rhythm is ascribed a prefrontal and medio-temporal control function in memory processes (Anderson et al., 2010; Buzsáki, 1996), the present study adds to recent evidence for a bottom-up mechanism of the theta-gamma code in the visual cortical networks (Landau et al., 2015; Lowet et al., 2016). The prefrontal, the hippocampal, the oculomotor and the visual cortical system may implement an mnemonic sampling loop. Novel perceptual information, reflected in gamma bursts, may be sampled bit by bit, at a theta pace (Fries, 2015), in order to integrate them into existing representations in neuronal networks. Such an mnemonic sampling mechanism may establish a continuous update of internal representations to the present state of the outer world (Buzsáki, 1996). Specifically, theta-gamma PAC provides an optimal temporal code for long-term potentiation processes in the medial temporal lobe (Pavlides et al., 1988), the core system for episodic memories (Eichenbaum, 2004; Squire and Zola-morgan, 1991), which may establish a coherent representation of time and space (Eichenbaum, 2017).

The present study provides a proof of concept that simplistic external pacemakers can entrain rhythmic processes in cortical networks and thereby entrain complex cognitive functions, such as memory encoding, in the wake human brain.

Acknowledgments

We thank Linda Zurlutter for her support in the data assessment and Nikolai Axmacher and Malte Wöstmann for providing comments on an earlier version of the manuscript.

Materials and Methods

Subjects

20 university students (19 females, M_{age} = 21.7, SD_{age} = 3.6) voluntarily participated and received monetary reward or course credits. None of the subjects reported any history of neurologic or psychiatric disorders and all subjects had normal or corrected to normal visual acuity. Informed consent was obtained from all subjects and the experimental procedure agreed with the World Medical Association's Declaration of Helsinki. All participants were included in the analyses.

Stimuli and Procedure

Individual frequency adjustment. We conducted a pre-study to identify individual theta and alpha frequencies, for procedural details see (Friese et al., 2013). In the pre-study subjects saw 300 colored object pictures and made living/nonliving judgements. Individual frequencies were then selected based on the grand mean of each participant (all trials of all conditions). Mean frequencies for 20 subjects that returned to the lab for the main study were 5.4 Hz (SD = 1.1 Hz) for theta and 10.2 Hz (SD = 1.7 Hz) for alpha. We also used the pre-study to determine the gamma range, peaking at 50 – 80 Hz over posterior electrodes.

Stimuli. The stimuli were 600 colored object pictures (e.g. plants, animals, clothes, tools), taken from a standard library (Hemera Photo Objects). Pictures were presented at the center of a 19 in. computer screen at a visual angle of about 6.2 × 6.2°.

Experimental paradigm. During encoding subjects saw 450 objects, presented in one of three conditions: individual theta, individual alpha, or static, presented in a random order. In the theta and alpha conditions, the object was presented at the individual frequencies determined in the pre-study (see above) by controlling the presentation at every refresh cycle of a 72 Hz CRT monitor (one refresh cycle = 13.89 ms). For example, to establish a flicker rate of 6 Hz, the object was presented at a duty cycle of 6:6, i.e. six on and six off cycles. Each picture was presented following a black screen (1 s) and a white fixation dot (variable duration of 0.5 – 1 s), for 3 s, ending at a full duty cycle.

To maintain attention during the whole stimulus presentation, subjects had to detect a magenta-colored dot that appeared for 111 ms on 15% of the encoding trials at a random time and position and respond as quickly as possible by a button press. These stimuli were not presented during retrieval and excluded from further analyses.

The retrieval phase followed a 15 min. filler task (solving simple math equations). 405 pictures from encoding were randomly intermixed with 150 new stimuli. Objects were presented for 2 s and subjects judged whether they would remember an object explicitly, with

details from encoding (“remember”), the object seemed familiar (“know”), or the object was novel to them (“new”), i.e., remember/know paradigm; (Tulving, 1995).

Behavioral analysis. Given the within-subject design, we compared the pure response rates of the three stimulation conditions: subsequently remembered (SR), subsequently known (SK), and subsequently forgotten (SF) responses. Note that the response rates do not need to be corrected by false alarm rates due to the within design. Our main comparison relied on the SR and SF responses and the subsequent memory effect (SME = SR-SF) for the theta and the alpha stimulation. Given the clear direction of the hypothesis that theta SSVEPs would lead to a higher SME than alpha SSVEPs, a one-sided test was applied for this main comparison. We quantified the overall memory entrainment effect (theta SME – alpha SME), to test if memory entrainment would be explained by the theta or the alpha stimulation. Theta and alpha SSVEPs were summarized by a mean z-score of the SSVEP signal at the peak electrode and the spread of the SSVEP signal across the scalp (across all 128 electrodes; Shannon entropy on SSVEP values, normalized from 0 to 1).

Electroencephalogram (EEG) Apparatus and Analysis

Apparatus. EEG was recorded from 128 active electrodes using a BioSemi Active-Two amplifier system at 512 Hz, in a electromagnetically-shielded room. Two additional electrodes (CMS: Common Mode Sense and DRL: Driven Right Leg; cf. http://www.biosemi.com/faq/cms&drl.htm) served as reference and ground.

Preprocessing. EEG signals were band-pass filtered from 1 Hz to 120 Hz and segmented into epochs from -1500 ms to 4500 ms, regarding the stimulus onset. Eye-blinks and muscle artifacts were detected using an independent component procedure and removed after visual inspection. Noisy trials were identified visually and discarded (approx. 5 % - 10 %). We applied a correction of saccade-related transient potentials (Hassler et al., 2011) to remove artifacts caused by miniature eye-movements (Yuval-Greenberg et al., 2008), before signals were re-referenced to the average reference.

Steady state visually evoked potentials (SSVEPs). The main analyses focused on the SSVEPs elicited by the theta and alpha stimulation. Specifically, the evoked spectral power was obtained by Morlet’s wavelets with approximately seven cycles at a resolution of 0.5 Hz for theta and alpha and a 2.0 Hz resolution in the gamma range. We identified the individual theta and alpha peak SSVEP signals, based on the grand mean spectral activity, and used the gamma range of 50-80 Hz, identified in the pre-study. Event-related changes for each condition and frequency were then calculated as the relative signal change of the post stimulus spectral activity, in percent, relative to a 500-250 ms for low frequencies, or 200-100

ms for gamma. For the analysis of theta and alpha SSVEPs as well as the gamma power in the SSVEP conditions, the SSVEP peak electrode of each condition was used (Figure 2).

Phase-amplitude coupling (PAC). To assess PAC between the phase of both low frequencies, theta and alpha, and the gamma amplitude (illustrated in Figure 3B), the modulation index (MI) (Canolty et al., 2006) was calculated as described previously (Friese et al., 2013). Specifically, the individual theta and alpha SSVEPs at the occipital peak electrode were filtered +/- 0.5 Hz around the individual peak frequency, and the 50-80 Hz filtered gamma signal, at all 128 electrodes. The MI was then calculated between the theta phase of the peak electrode in combination with the gamma amplitude, separately for each electrode, for the 500-3000ms time window. With the same procedure and using the same electrodes, we tested theta-gamma PAC across a 40-120Hz gamma range, in 5Hz steps, using a 20Hz sliding window for the gamma frequency, separated between conditions. The resulting MI value was averaged across all electrodes. For a circular plot of the subsequent memory differences (SR-SF) for gamma amplitudes, we z-standardized the gamma amplitudes across the 18 bins for each participant and condition. The SME difference (SR-SF) in standardized gamma amplitudes was averaged over the left temporal peak electrodes of the MI difference plot (Figure 2B).

References

Anderson, K.L., Rajagovindan, R., Ghacibeh, G.A., Meador, K.J., and Ding, M. (2010). Theta oscillations mediate interaction between prefrontal cortex and medial temporal lobe in human memory. Cereb. Cortex *20*, 1604–1612.

Bahramisharif, A., Jensen, O., Jacobs, J., and Lisman, J. (2017). Serial representation of items during working memory maintenance at letter-selective cortical sites. bioRxiv.

Buzsaki, G. (2004). Neuronal Oscillations in Cortical Networks. Science. *304*, 1926–1929.

Buzsáki, G. (1996). The hippocampo-neocortical dialogue. Cereb. Cortex *6*, 81–92.

Canolty, R.T., Edwards, E., Dalal, S.S., Soltani, M., Nagarajan, S.S., Kirsch, H.E., Berger, M.S., Barbaro, N.M., and Knight, R.T. (2006). High Gamma Power Is Phase-Locked to Theta Oscillations in Human Neocortex. Science. *313*, 1626–1628.

Cowan, N. (1988). Evolving Conceptions of Memory Storage, Selective Attention, and their Mutual Constraints Within the Human Information-Processing System. Psychol. Bull. *104*, 163–191.

Eichenbaum, H. (2004). Hippocampus: Cognitive processes and neural representations that underlie declarative memory. Neuron *44*, 109–120.

Eichenbaum, H. (2017). Perspective On the Integration of Space , Time , and Memory. Neuron *95*, 1007–1018.

Engel, A.K., Fries, P., and Singer, W. (2001). Dynamic predictions: Oscillations and synchrony in top–down processing. Nat. Rev. Neurosci. *2*, 704–716.

Fell, J., and Axmacher, N. (2011). The role of phase synchronization in memory processes. Nat. Rev. Neurosci. *12*, 105–118.

Fries, P. (2015). Rhythms for Cognition: Communication through Coherence. Neuron *88*, 220–235.

Friese, U., Köster, M., Hassler, U., Martens, U., Trujillo-Barreto, N., and Gruber, T. (2013). Successful memory encoding is associated with increased cross-frequency coupling between frontal theta and posterior gamma oscillations in human scalp-recorded EEG. Neuroimage *66*, 642–647.

Hanslmayr, S., Staresina, B.P., and Bowman, H. (2016). Oscillations and Episodic Memory:

Addressing the Synchronization/Desynchronization Conundrum. Trends Neurosci. *39*, 16–25.

Hassler, U., Barreto, N., and Gruber, T. (2011). Induced gamma band responses in human EEG after the control of miniature saccadic artifacts. Neuroimage.

Heusser, A.C., Poeppel, D., Ezzyat, Y., and Davachi, L. (2016). Episodic sequence memory is supported by a theta–gamma phase code. Nat. Neurosci. *19*, 1374–1380.

Jensen, O., and Mazaheri, A. (2010). Shaping Functional Architecture by Oscillatory Alpha Activity: Gating by Inhibition. Front. Hum. Neurosci. *4*, 1–8.

Kandel, E.R., Schwartz, J.H., and Jessell, T.M. (2013). Principles of Neural Science.

Klimesch, W. (1999). EEG alpha and theta oscillations reflect cognitive and memory performance: A review and analysis. Brain Res. Rev. *29*, 169–195.

Klimesch, W. (2012). Alpha-band oscillations, attention, and controlled access to stored information. Trends Cogn. Sci. *16*, 606–617.

Landau, A.N., Schreyer, H.M., Van Pelt, S., and Fries, P. (2015). Distributed Attention Is Implemented through Theta-Rhythmic Gamma Modulation. Curr. Biol. *25*, 2332–2337.

Lisman, J.E., and Jensen, O. (2013). The Theta-Gamma Neural Code. Neuron *77*, 1002–1016.

Lowet, E., Roberts, M.J., Bosman, C.A., Fries, P., and de Weerd, P. (2016). Areas V1 and V2 show microsaccade-related 3-4-Hz covariation in gamma power and frequency. Eur. J. Neurosci. *43*, 1286–1296.

Marshall, L., Helgadóttir, H., Mölle, M., and Born, J. (2006). Boosting slow oscillations during sleep potentiates memory. Nature *444*, 610–613.

Müller, M., Malinowski, P., Gruber, T., and Hillyard, S. (2003). Sustained division of the attentional spotlight. Nature.

Ngo, H.V. V, Martinetz, T., Born, J., and Mölle, M. (2013). Auditory closed-loop stimulation of the sleep slow oscillation enhances memory. Neuron *78*, 545–553.

O'Keefe, J., and Recce, M.L. (1993). Phase relationship between hippocampal place units and the EEG theta rhythm. Hippocampus *3*, 317–330.

Osipova, D., Takashima, A., Oostenveld, R., Fernandez, G., Maris, E., and Jensen, O. (2006). Theta and Gamma Oscillations Predict Encoding and Retrieval of Declarative Memory. J.

Neurosci. *26*, 7523–7531.

Paller, K.A., and Wagner, A.D. (2002). Observing the transformatioin of experience into memory. Trends Cogn. Sci. *6*, 93–102.

Pavlides, C., Greenstein, Y.J., Grudman, M., and Winson, J. (1988). Long-term potentiation in the dentate gyrus is induced preferentially on the positive phase of θ-rhythm. Brain Res. *439*, 383–387.

Squire, L.R., and Zola-morgan, S. (1991). The Medial Temporal Lobe Memory System. Science. *253*, 1380–1386.

Staudigl, T., and Hanslmayr, S. (2013). Theta oscillations at encoding mediate the context-dependent nature of human episodic memory. Curr. Biol. *23*, 1101–1106.

Tulving, E. (1995). Organization of Memory: Quo Vadis? Cogn. Neurosci. 839–847.

Varela, F., Lachaux, J., Rodriguez, E., and Martinerie, J. (2001). The brainweb: phase synchronization and large-scaleintegration. Nat. Rev. Neurosci. *2*, 229–239.

Yuval-Greenberg, S., Tomer, O., Keren, A.S., Nelken, I., and Deouell, L.Y. (2008). Transient Induced Gamma-Band Response in EEG as a Manifestation of Miniature Saccades. Neuron *58*, 429–441.